PRACTICAL AND APPLIED MEDICAL PHYSICS

CLINICAL COMPARISON OF DENSITY CORRECTION METHODS ASSOCIATED WITH PENCIL BEAM CONVOLUTION ALGORITHM FOR CLINICAL SITUATIONS

Abdulhamid Chaikh[1,2] , Jean-Yves Giraud[1,2], Jacques Balosso[1,2]

[1] University Joseph Fourier, Grenoble, France
[2]Department of Radiation Oncology and Medical physics, Grenoble University Hospital, France

Abstract- **Purpose: the aim of this work was to quantify and assess the differences in dose computed using density correction methods integrated into the Pencil Beam Convolution (PBC) algorithm for planning target volumes and organs at risk. Methods and materials: 12 patients including 7 chest cancers, 2 head and neck cancers, 2 brain cancers and 1 prostate cancer were analysed. For each patient, 3 treatment plans were generated using exactly the same beam configurations. For plans 1, 2 and 3 the dose was calculated using Modified Batho method (PBC-MB), Batho Power Law method (PBC-BPL) and Equivalent Tissue Air Ratio method (PBC-ETAR), respectively. To evaluate the treatment plans, the monitor units, isodose curves, dose volume histograms, quality indexes and gamma indexes were compared. A statistical analysis was performed using the Wilcoxon signed rank test. Results: the difference in monitor units using PBC-BPL was 1.6% (SD : 2.5) for lung and less than 1% for head and neck, brain and prostate. This difference was less than 1% for all sites using PBC-ETAR. The Wilcoxon test showed a statistically significant difference between PBC-MB and PBC-BPL only for chest ($p < 0.01$). There was a statistically significant difference between PBC-MB and PBC-ETAR for chest ($p = 0.02$), head and neck ($p = 0.02$) and brain ($p = 0.02$). For dose volume histograms the difference between density correction methods was less than 1.1%. Wilcoxon test showed only a significant difference for minimum dose using PBC-BPL. The three density correction methods showed similar quality ($p > 0.05$). 2D gamma analysis showed all pixels with gamma ≤ 1. Conclusion: the density correction methods based on 1D using PBC-BPL and PBC-MB produced a dose distribution close to PBC-ETAR which calculates the density correction in 3D. Therefore, we propose the use of the Modified Batho method to calculate the delivered dose.**

Key words: **density correction, PBC, Modified Batho, Batho Power Law, Equivalent TAR**

I. INTRODUCTION

The aim of radiotherapy is to deliver the prescribed dose to the tumour with a minimum dose to the surrounding healthy tissues. The International Commission on Radiation Units and Measurements (ICRU report No. 50, 1993 and report No. 62, 1999) recommends the dose to be delivered should be within ± 5% of the prescribed dose [1,2]. The dose calculation can be performed using different algorithms. These algorithms play a key role in treatment planning systems (TPS). The TPS Eclipse® (Version 8.1; Varian Medical Systems, Palo Alto, CA) incorporates the Pencil Beam Convolution (PBC) algorithm. The PBC algorithm includes three density correction methods for dose calculation in order to take into account the heterogeneity of tissues. The objective of this study was to compare the different density correction methods implemented in the PBC algorithm in terms of their ability to calculate the delivered dose in Monitor Units (MUs) and the dose distribution under a variety of clinical situations.

II. MATERIAL AND METHODS

A. Dose calculation algorithm

In this study, the dose calculation was performed using the PBC algorithm incorporated in the Eclipse® TPS. The PBC algorithm is based on a pencil beam kernel convolution and computes the dose to the patient as the superposition of the total energy released per mass unit within an energy deposition kernel. The kernel represents the spread of energy from the primary photon interaction site throughout the volume. To model the heterogeneity, the kernels vary with electron density based on the electron

density scaling theorem. Heterogeneity corrections are always based on relative electron densities obtained from a CT-Scan. Calculations with density correction were performed using three density correction methods: Batho Power Law (PBC-BPL), Modified Batho (PBC-MB) and Equivalent Tissue Air Ratio (PBC-ETAR). This process involved two stages: first, a relative dose distribution was calculated within a medium of homogeneous water–equivalent composition, and then an Inhomogeneity Correction Factor (ICF) was added. This factor makes adjustments to the uncorrected distribution to account for variations in tissue density [3,4,5,6,7,8]. The ICF is thus defined as:

ICF= Dose in heterogeneous medium divided by Dose at the same point in homogenous medium (1)

Batho Power Law method: this method was proposed by Batho in 1964 and then generalized by Sontag and Cunningham. It calculates the density distribution in one dimension 1D. The correction factor is given by:

$$ICF = \prod_{m=1}^{m=N} TAR(X_m)^{(\rho_m-\rho_{m-1})/\rho_0 (\mu_{en}/\rho)_N/(\mu_{en}/\rho)_W} \quad (2)$$

Where: N is the number of layers of different densities above the point of calculation, m: layer number, X_m: distance from point of interest to the surface of the m^{th} layer. ρ_m and ρ_0 are the electron densities of the m^{th} layer and that of water, respectively. $(\mu_{en}/\rho)_N$ and $(\mu_{en}/\rho)_w$ are the mass energy absorption coefficients of the material in layer N and that of water, respectively.

Modified Batho method: this method is based on the Tissue Maximum Ratio (TMR) and calculates the density distribution in 1D. The correction factor is given by:

$$ICF = (\mu_{en}/\rho)_N/(\mu_{en}/\rho)_W \prod_{m=1}^{N} (TMR(z-z_m+z_{bu}))^{(\mu_m-\mu_{m-1})/\mu_w} \quad (3)$$

where μ_m and μ_w are the linear attenuation coefficients of the material in layer m and water respectively; Z_{bu} is the build-up depth and Z_m is the distance along the beam from the surface to the layer m in the phantom.

Equivalent Tissue Air Ratio method: this method calculates the density distribution in 3D and uses full CT information to account for scattered radiation. It uses the Tissue Air Ratio **(**TAR) dependent on the effective beam radius ($\tilde{r}$) to take account of scattered radiation and effective depth (d') for primary beam correction. The correction factor is given by:

$$ICF = \frac{TAR\ (d', \tilde{r})}{TAR\ (d, r)} \quad (4)$$

where $d', \tilde{r}$: are the effective values of depth (d) and beam radius (r) respectively.

B. Treatment plan design

For each patient, 3 treatment plans were generated using exactly the same configuration of beams, collimator and accessories. The doses in plans 1, 2 and 3 were calculated using PBC-MB, PBC-BPL and PBC-ETAR, respectively. In all plans, the dose was prescribed at a single reference point, as recommended by ICRU. The dose using PBC-MB was taken as the reference plan and was the one used to treat the patients. The reference treatment plans were designed according to the clinical experience of the department and ICRU recommendations. For the Planning Target Volume (PTV), 95% of the prescribed dose encompassed the volume and the maximum dose within the PTV was under 107% of the prescribed dose. For organs at risk (OAR), the recommended dose constraints were respected.

C. Clinical cases

This study included 12 patients presenting a wide range of tumor types and cancer sites: 7 chests, 2 head and neck, 2 brains and 1 prostate. These patients were irradiated using 3D- Conformal Radiation Therapy. Table 1 shows the tumor location, the number of PTV, the total prescribed dose (Gy), and the number of fields and energies (MV) for each patient.

Table 1 The tumor location, PTV number, total prescribed dose, number of treatment fields and energies for each patient.

Patient	Site	PTV	Dose (Gy)	Fields	Energy MV
1	Chest	2	66	6	18
2	Chest	3	66	14	18
3	Chest	3	70	10	18
4	Chest	2	60	9	18
5	Chest	2	60	12	18
6	Chest	2	54	8	18
7	Chest	2	90	6	6
8	Head and neck	3	60.7	12	6
9	Head and neck	3	72	12	6
10	Brain	1	36	5	6
11	Brain	1	40.5	4	18 and 9
12	Prostate	2	70	10	18

D. Treatment plan evaluation

Dosimetric analysis: in order to evaluate the treatment plans, the following dosimetric parameters were used and compared:

MUs: for each patient and each field the MUs calculated using PBC-MB, PBC-BPL and PBC-ETAR in plan 1, 2 and 3 were compared.

Isodose curves: the 95% and 100% isodose curves inside the PTVs were compared.

Dose volume histogram (DVH): for each PTV, minimum dose, mean dose and maximum dose as well as the

calculated dose delivered to 95% of the PTV (D95) were compared.

Quality index: we used the Conformity Index (CI) defined as the ratio of the minimum dose encompassing the PTV to the prescribed dose, to compare the plan conformity. We used the Homogeneity Index (HI), defined as the ratio of the maximum dose to the PTV to the prescribed dose, to compare the homogeneity dose for PTV. The PTV Conformity Index (CI_{PTV}), defined as the PTV volume receiving more than 95% of the prescribed dose divided by the PTV volume, was used to compare the degree of conformity of the prescribed dose. We used the geometrical index (g) to compare the geometric conformity to PTV and normal tissues, where $g = (V_{PTV} + V_{NT}) / PTV$ volumes. V_{PTV} designates the PTV volumes receiving a dose less than 100% of the prescribed dose. V_{NT} are the normal tissue volumes receiving 100% of the prescribed dose [9,10].

Global analysis: the gamma index was introduced by Low et al [11]. In this study, a 2D gamma index was used to compare the dose distribution using the CT-Scan image including PTV and the OAR. The DICOM image for each patient was exported from TPS Eclipse® to RIT-113® (Radiation Dosimetry Systems, Version 5.2). The matrix center was aligned with the isocenter. The dimensions used were 20x20cm². For this study, the gamma criterion was set at 3% for the dose and 3mm for the "Distance to Agreement". The 2D gamma analysis was displayed using a gamma plot and gamma pixel histogram indicating the fraction of pixels with a gamma index equal or below a specific value. A mean value of gamma ≤ 1 indicates agreement between dose distributions. We considered that the dose distribution using PBC-MB agreed with the dose distribution calculated with PBC-BPL or PBC-ETAR if 95% of pixels had gamma ≤ 1.

Statistical analysis: Wilcoxon signed rank test was used to assess the statistical significance of differences. Language R® (version 2.15.2/2012-10-26) was employed to calculate *p*-values with an alpha error equal to 5%. A *p*-value < 0.05 was considered as statistically significant. Data are presented as Mean ± Standard Deviation (SD).

III. Results

MUs: Table 2 summarizes the dosimetric and statistical results for the MUs. It can be seen that the Wilcoxon test showed a statistically significant difference between PBC-MB and PBC-BPL only for the chest. The comparison between PBC-MB and PBC-ETAR showed that the difference was statistically significant for chest, head and neck, and brain. Figure 1 shows the beams distribution as a function of difference in MUs (%) for all fields.

Table 2 Dose difference in MUs between PBC-MB and PBC-BPL or PBC-ETAR for plans 1, 2 and 3; *p*-value: using Wilcoxon signed rank test; SD: Standard Deviation.

Patient	MB *vs* BPL		MB *vs* ETAR	
	Mean ±SD	*p*-value	Mean ±SD	*p*-value
Chest	1.6±2.5	< 0.01	0.2±2.1	0.03
Head and neck	0.1±1.1	0.5	0.7±1.4	0.02
Brain	0.4±0.6	0.2	0.6±1.2	0.02
Prostate	0.2±1.1	0.7	0.1±0.7	1

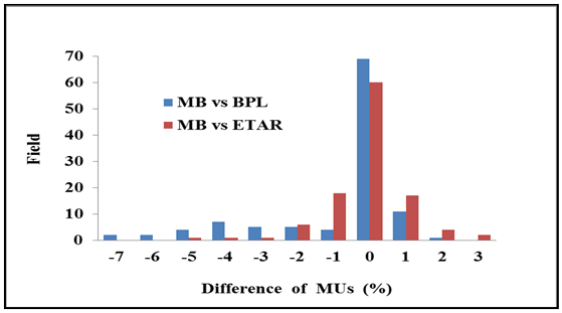

Fig. 1 Beam distribution as a function of difference in MU for all fields.

Isodose curves: there was no hot spot either in normal tissues or within the PTV in any treatment plan. In the transverse plan, we found that the 95% line calculated by the three density correction methods included the whole PTV whatever its location. There was no difference in the 100% isodose curves. Figure 2 shows the transverse views of isodose distribution curves for plan 1, 2 and 3 with heterogeneity correction.

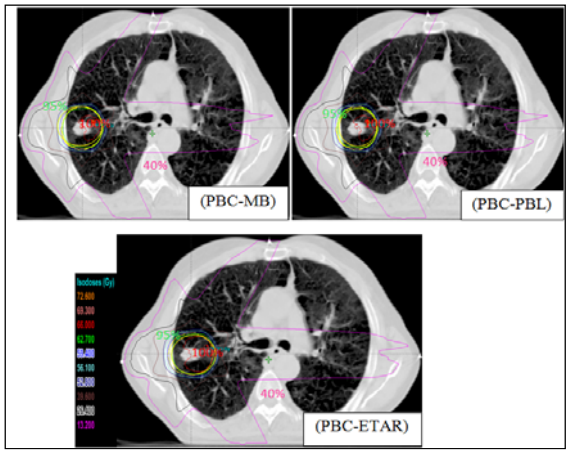

Fig. 2 Transverse views of isodose distribution curves for plan 1, 2 and 3 using density correction methods: PBC-MB, PBC-BPL and PBC-ETAR, respectively. A dose of 66Gy was prescribed at isocenter for lung in plans 1, 2 and 3. Yellow colouring shows the PTV. Red, green and orange colouring show100%, 95% and 40% isodose curves, respectively.

DVH: Table 3 summarizes the dosimetric and statistical results for PTV. It can be seen that the difference between PBC-MB and PBC-BPL was less than 1.1%, but the

difference between PBC-MB and PBC-ETAR was less than 0.6% for all sites. Figure 3 shows the DVH for lung using the three density correction methods.

Table 3 Dose volume parameters for planning target volume for all patients. D95: the calculated dose delivered to 95% of the PTV volume; *p*-value: Wilcoxon signed rank test; SD: Standard Deviation.

Plans	Dose	Minimum dose	Mean dose	D95	Maximum dose
BPL	Mean ±SD	1.1±1.2	0.1±0.7	0.9±2.3	0.6±1.1
	p-value	0.001	0.4	0.06	0.05
ETAR	Mean ±SD	0±2.6	0.2±1.1	0.5±1.7	0.6±1.2
	p-value	0.43	0.1	0.6	0.1

Quality indexes: Table 4 summarizes the quality indexes for all patients using the three density correction methods. A Wilcoxon test showed that there was no statistically significant difference between all indexes, ($p > 0.05$).

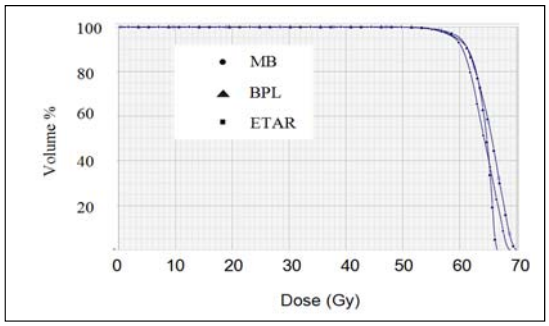

Fig. 3 Cumulative dose volume histograms for PTV located in lung. The histograms were calculated by PBC- MB, PBC-BPL and PBC-ETAR for plans 1, 2 and 3 respectively.

Table 4 Quality index for all patients using PBC-MB, PBC-BPL and PBC-ETAR for plans 1, 2 and 3 respectively. CI: Conformity Index; HI: Homogeneity Index; CI_{PTV}: Conformity Index for planning target volume and g: geometrical index; *p*-value: Wilcoxon signed rank test; SD: Standard Deviation.

	Index	CI	HI	CI_{PTV}	g
MB	Mean ±SD	0.8±0.2	1.1±0.04	0.8±0.2	0.2±0.2
BPL	Mean ±SD	0.8±0.2	1.1±0.04	0.8±0.2	0.2±0.2
	p-value	1	0.3	0.2	0.2
ETAR	Mean ±SD	0.8±0.2	1.1±0.04	0.8±0.2	0.2±0.2
	p-value	1	0.09	0.6	0.05

Global analysis: 2D gamma analysis showed that the mean values of gamma were less than unity using PBC-BPL and PBC-ETAR, compared to PBC-MB. The results for the gamma pixel histograms showed that the 95% of pixels had gamma ≤ 1 using the set criteria (3%, 3mm). Figure 4 shows 2D gamma plots in the traverse plane, comparing PBC-MB with PBC-BPL and PBC-ETAR for chest cancer. The gamma plot was calculated in 2D using DICOM images including the PTV and OAR. The rectangles in figure 4 show the PTV and the red shading indicates that gamma values were unity (outside tolerance limits). We note a small area with gamma >1 using PBC-BPL, but using PBC-ETAR all pixels had gamma <1. Figure 5 shows the 2D gamma pixel histograms obtained from the comparison between PBC-MB and PBC-BPL and PBC-ETAR for chest cancer. In this case we note that the condition of 95% of pixels with gamma ≤ 1 is satisfied.

IV. Discussion

There is a wide variety in the algorithms used to apply density corrections. The report of Task Group No.65 of the Radiation Therapy Committee of the American Association of Physicists in Medicine has classified the density correction methods into two general categories according to:

- the description of the density correction (1D or 3D)
- the inclusion or exclusion of electron transport

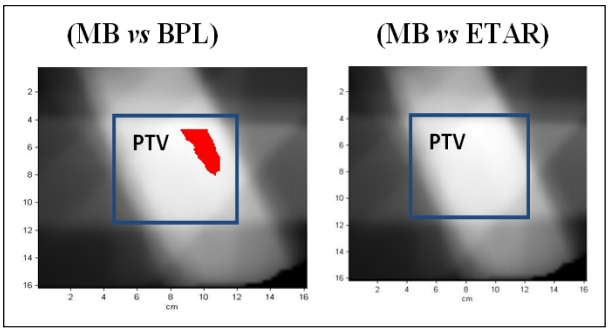

Fig. 4 gamma plot in 2D comparing PBC-MB with PBC-BPL, and with PBC-ETAR for chest cancer. The gamma plot was calculated in 2D using DICOM images including the PTV and OAR. We note that there was a small area with gamma >1 in the PTV using PBC-BPL, but all pixels had gamma <1 using PBC-ETAR.

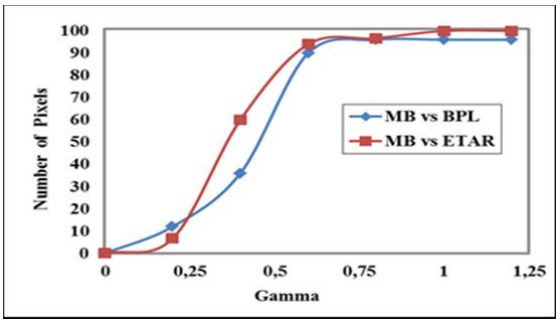

Fig.5 Gamma pixels histograms in 2D obtained from the comparison between PBC-MB with PBC-BPL and PBC-ETAR for chest cancer. In this case we note that the condition of 95% of pixels with gamma ≤ 1 is satisfied.

In this study three density correction methods that are frequently integrated into the PBC algorithm were used. None of these methods take into account the changes in lateral electron transport. The modified Batho method is based on an empirical correction factor that uses TMR and calculates the dose in 1D. The Batho Power Law method applies a correction factor using TAR and calculates the dose in 1D. The ETAR method calculates the dose in 3D. In this study for simple heterogeneous tissues such as head and neck, brain and prostate, there was no statistically significant difference between MU results for PBC-MB and PBC-BPL, but the difference was highly significant for chest ($p < 0.01$). This suggests that the low density nature of lung tissue influences the dose distribution. Using the PBC-ETAR method the difference was statistically significant for chest, head and neck and brain. For tumors located in high density tissues such as the prostate the three density correction methods calculated the same MUs, ($p = 1$). The inaccuracy between the density correction methods is due to the nature of the correction factor, which influences the dose calculation. However, all three methods showed the same quality indexes for all clinical cases, as shown in Table 4. The global analysis, based on 2D gamma, showed that the three density correction methods calculated the same dose distribution for each patient including PTV and OAR. In all cases the mean values of gamma were less than unity and 95% of pixels had gamma ≤ 1. We observed that the PBC-MB method currently offers the best compromise between under dosage and over dosage for PTV. Therefore, in our department we propose this method to calculate the dose for all cancers whatever the site.

V. Conclusion

In this study we compared the density correction method PBC-MB with PBC-BPL and with PBC-ETAR. We generated 3 treatment plans for 12 patients presenting a wide range of tumor types and sites. The inaccuracy between density correction methods was 1.6% for MUs and 1% for DVH. However, the methods showed similar quality indexes ($p > 0.05$). We propose that the Modified Batho method PBC-MB is used to calculate the delivered dose.

References

1. ICRU Report No. 50. Prescribing, Recording and Reporting Photon BeamTherapy. International Commission on Radiation Units and Measurements, Bethesda, Maryland, 1993.
2. ICRU Report No. 62. Prescribing, Recording and Reporting Photon Beam Therapy supplement to ICRU Report 50, International Commission on Radiation Units and Measurements, Bethesda, Maryland, 1999.
3. Task Group No. 65, the Radiation Therapy Committee of the American Association of Physicists in Medicine. Tissue inhomogeneity corrections for MV photon beams. Madison, WI: Medical Physics Publishing, 2004.
4. Ahnesjö A, Aspradakis M M. Dose calculations for external photon beams in radiotherapy. Phys. Med. Biol. 1999; 44 : 99–155.
5. Batho H F. Lung corrections in cobalt 60 beam therapy. J Can Assoc Radiol 1964; 15:79-83.
6. El-Khatib E, Battista J J. Improved lung dose calculation using tissue-maximum ratios in the Batho correction. Med Phy.s 1984;11 (3):279–286.
7. Thomas S J. A modified power-law formula for inhomogeneity corrections in beams of high energy x rays. Med. Phys. 1991; 18, 719 -723.
8. Wong J W, Purdy J A. On methods of inhomogeneity corrections for photon transport. Med Phys. 1990; 17(5):807-14.
9. Feuvret L, Noël G, Nauraye C, Garcia P, Mazeron J J. Conformal index and radiotherapy. Cancer/Radiothérapie. 2004; 8: 108–119.
10. Lomax N J, Scheib S G. Quantifying the degree of conformity in radiosurgery treatment planning. Int J Radiat Oncol Biol Phys. 2003; 55:1409–19.
11. Low DA, Harms WB, Mutic S, Purdy JA. A technique for the quantitative evaluation of dose distributions. Med Phys. 1998; 25(5):656–61.

Contacts of the corresponding author:

Author: Abdulhamid Chaikh
Institute: Department of Radiation Oncology and Medical physics, Grenoble University Hospital, France
Street: CS 10217 C.H.U de Grenoble 38043
City: Grenoble
Country: France
Email: abdulhamedc@yahoo.com

Conflict of Interest : None